A Starch-Based Biodegradable Film Modified by Nano Silicon Dioxide

Huali Tang, Hanguo Xiong, Shangwen Tang, Peng Zou

College of Food Science and Technology, Huazhong Agricultural University, Wuhan, Hubei 430070, People's Republic of China

Received 5 September 2007; accepted 5 December 2008
DOI 10.1002/app.29855
Published online 13 March 2009 in Wiley InterScience (www.interscience.wiley.com).

ABSTRACT: The purpose of this work was to improve the properties of the starch/poly(vinyl alcohol) (PVA) films with nano silicon dioxide (nano SiO_2). Starch/PVA/nano-SiO_2 biodegradable blend films were prepared by a solution casting method. The characteristics of the films were assessed by Fourier Transform infrared spectroscopy (FTIR), scanning electron microscopy (SEM), and X-ray photoelectron spectroscopy (XPS). The results obtained in this study indicated that the nano-SiO_2 particles were dispersed evenly within the starch/PVA coating and an intermolecular hydrogen bond and a strong chemical bond C—O—Si were formed in the nano-SiO_2 and starch/PVA. That the blending of starch, PVA and nano-SiO_2 particles led to uniform starch/PVA/nano-SiO_2 blend films with better mechanical properties. In addition, the nano-SiO_2 particles can improve the water resistance and light transmission of the blend films. © 2009 Wiley Periodicals, Inc. J Appl Polym Sci 113: 34–40, 2009

Key words: biodegradable film; nano silicon dioxide; corn starch; structure; properties

INTRODUCTION

The use of biodegradable polymers for packaging offers an alternative and partial solution to the problem of accumulation of solid waste composed of synthetic inert polymers.[1,2] Starch, as an abundant and inexpensive raw material, has been applied in the field of biomaterials.[3,4] However, packaging films (composed entirely of starch) lack the strength and rigidity to withstand the stresses to which many packaging materials are subjected.[5]

Nano-SiO_2 is a kind of amorphous powder with a tridimensional net molecular structure. It deviates from a stable silicon-oxygen structure because of a lack of oxygen on its surface. Its molecular formula is SiO_{2-x}, with x ranging from 0.4 to 0.8. Because of its small size, large specific surface area, high surface energy, and unsaturated chemical bonds and hydroxyl groups on the surface, Nano-SiO_2 is easy to disperse among the macromolecular chains. Many studies indicated that nanomaterials can improve and enhance the performance of polymer materials such as plastic and rubber,[6–9] but a relevant study on the starch polymers modified by nano-SiO_2 has not been reported yet. Nano-SiO_2 can be used to modify starch because of its properties of multihydroxy and high surface activity. The interpenetrating network structure of nano-SiO_2/starch hybrid materials are formed by combining the stiff structure of nano-SiO_2 with the flexible structure of starch.

Poly(vinyl alcohol) (PVA) is a biodegradable synthetic material which has the advantages of good film forming, strong conglutination, and high thermal stability. In recent years, PVA has widely used in the materials industry.[10–15] In this experiment, the tensile strength and elongation at break of starch film were further enhanced and improved by adding the appropriate PVA. By studying the effect of nano-SiO_2 on the structure and properties of starch film in our laboratory, we were able to discover the mechanism for improving the properties of a starch-based biodegradable film using nano-SiO_2.

EXPERIMENTAL

Materials

Nano silicon dioxide (nano-SiO_2), with a particle size of 30 nm, was provided by the Nanometer Engineering Center of the People's Republic of China. The corn starch (starch) was provided by Huanglong Food Ltd. of Gongzhuling City (moisture content 11.7%, protein 0.23%, fat 0.075%, and ash content 0.08%). The polyvinyl alcohol (PVA) was produced and provided by Chongqing Inorganic Chemical Reagent Factory (DP 1799 $\pm$ 50, NaOH $\leq$ 0.2%, acetic acid remnant $\leq$ 0.13%, volatilization content $\leq$ 9.0%,

Correspondence to: H. Xiong (xionghanguo@163.com).

and transmissivity $\geq$ 90%). hexamethylene tetramine, glycerine, Tweenum-80, liquid paraffin, and other reagents were all analytical grade and were used as received.

Sample preparation

Preparation of starch/PVA (SP) films

Six grams of starch and 4 g of PVA were poured into a round bottom flask with 100 mL deionized water and stirred with motor stirrer (JJ-1, Changzhou, China) at high-speed in a constant temperature water bath at 95°C for 20 min (>1000 rpm). Next, 0.1 g of hexamethylene tetramine was added as a crosslinker and stirring was continued for 40 min (>1000 rpm), then, 1.5 g of glycerine as plasticizers, 0.6 g of tweenum-80 as surfactants, and 1.2 g of liquid paraffin as mold release agents were mixed in turn and the film-forming solutions were again continuously stirred for 10 min then cast onto a glass plate [20 cm × 20 cm] placed on a leveled flat surface. After the blends were allowed to dry at 95°C in an oven (101A-2, Shanghai, China) for 1 h, the films were then peeled off and reserved. The starch/PVA films were coded as SP.

Preparation of starch/PVA/nano-SiO_2 (SPN) films

Six grams of starch with different nano-SiO_2 contents (0.1 g, 0.2 g, 0.3 g, 0.4 g, and 0.5 g) were added into a bowl and milled for 1 h. It was mixed uniformly, and then the mixture and 4 g of PVA were poured into a round bottom flask with 100 mL deionized water, stirred for 5 min at high speed (>1000 rpm), then dispersed for 10 min by ultrasound (intermittent dispersion of pulsing on for 3 s and off for 2 s, with the frequency of 20 kHz). Afterwards, the mixture was stirred at high speed in a constant temperature water bath at 95°C for 20 min (>1000 rpm) and 0.1 g of hexamthylene tetramine was added. Stirring was continued for another 40 min (>1000 rpm), then 1.5 g of glycerine, 0.6 g of tweenum-80, and 1.2 g of liquid paraffin were mixed in turn while continuously stirring for 10 min. The mixture was cast onto a glass plate placed on a leveled flat surface. After the blends were allowed to dry at 95°C in an oven for 1 h, the films were peeled off and reserved. The films with different nano-SiO_2 contents were coded as SPN1, SPN2, SPN3, SPN4, and SPN5 in turn.

Film thickness measurement

The thickness of films was determined using a micrometer (Mitutoyo Corp., Code No. 543-551-1, Model ID-F125, Japan) to the nearest 0.001 mm at 10 random positions around the film, and average values were used in calculations.

Physical and biodegradable properties test

The tensile strength and elongation at break of the films were determined using the electron tensile tester CMT-6104 (Shenzhen Sans Test Machine Co., Ltd., China) according to the Chinese standard method GB/T 4456-96 (Polyethylene Blown film for packaging, 1996). The films were cut into 120 mm × 15 mm strips, with the gauge length (i.e., the distance between the two clamps) set at 80 mm, a tensile rate (i.e., the rate of extending travel of the clamp) of 250 mm/min, a return rate (i.e., the rate of return travel of the clamp) of 200 mm/min, and a breaking load of 200*N*.

The 80 mm ×80 mm sheet film was weighed (W_0) and immersed in 25°C water for 10 min. Then the wet film with filter paper to remove surface moisture and immediately weighed (W_1). The water absorption (Wa) were calculated using the following equation:

$$\mathrm{Wa}(\%) = (W_1 - W_0)/W_0 \times 100$$

The transmittance (T) of the prepared hybrid films ($\sim$ 0.2 mm thickness) was measured by using a Shimadzu UV-160A spectrophotometer (Shimadzu, Kyoto, Japan) in the wavelength range of 200–800 nm.[16]

The biodegradation rate of the film was according to the methods specified in IDT ISO 14855 : 1999.[17]

Characterization

The powdered samples were blended with potassium bromide and laminated, and the IR spectra were recorded with a Nicolet (USA) Nexus 470 FTIR spectrometer. The wave range, from 4000 cm^{-1} to 400 cm^{-1}, was scanned 32 times for spectrum integration. The scanning resolution was 16 cm^{-1}.

X-ray photoelectron spectroscopy (XPS) was conducted using a Perkin–Elmer PHI 5600 ESCA system. Setting the hydrocarbon peak maximum in the C_{1s} spectra to 284.6 eV referenced the binding energy scales for the samples.

The surface and cross section of the blend films were observed using a Philips XL-3 scanning electron microscope (SEM) with the accelerating voltage of 30 kV. All specimens were coated with gold and then observed at magnification 1000×.

RESULTS AND DISCUSSION

Physical properties

Mechanical properties

Because polymer materials may be subjected to various kinds of stress in the process of usage, the determination of the mechanical properties involves not

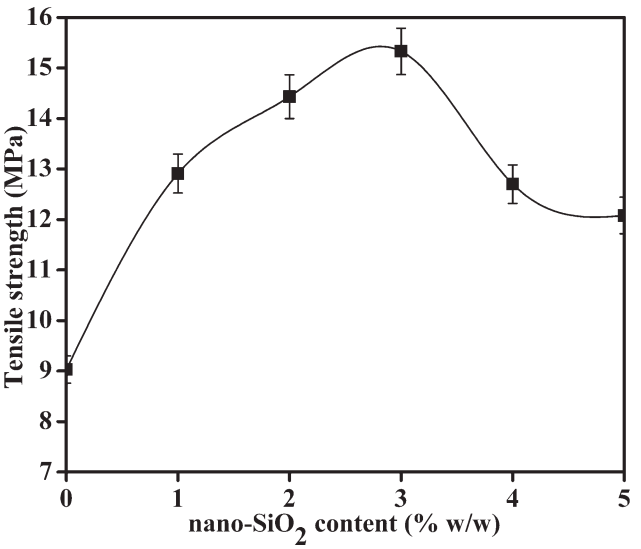

Figure 1 The dependence of tensile strength on the nano-SiO_2 content of blend films.

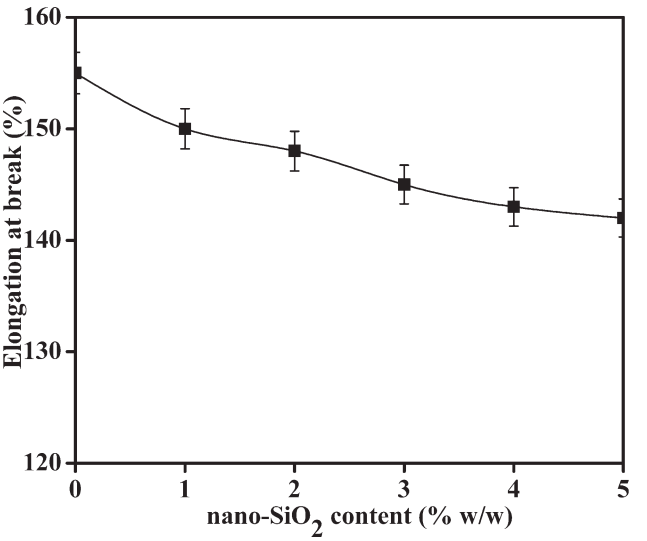

Figure 2 The dependence of the elongation at break on the nano-SiO_2 content of blend films.

only scientific but also technological and practical aspects.[18] The influence of the nano-SiO_2 content on the tensile strength of the blend films is shown in Figure 1. The tensile strength of the SP film was 9.03 MPa. When the nano-SiO_2 was added into the starch and polyvinyl alcohol blend solution, the tensile strength of the resulting blend film increased along with an increase of nano-SiO_2 content and reached a maximum point at about 3 wt % of the nano-SiO_2 content (SPN3), thus achieving 15.33 MPa. When the nano-SiO_2 content exceeded 3%, the tensile strength of the blend film decreased along with an increase of nano-SiO_2 content, but it was still higher than the SP film. A possible explanation of the previous phenomenon is that as nano-SiO_2 added to starch/PVA mixture, the intermoleculer interfacial adhesion is improved by the presence of intermolecular interactions between nano-SiO_2 and starch or nano-SiO_2 and polyvinyl alcohol in the blend films, which helps to strengthen starch/PVA chains, then, the tensile strength of the composites increased. However, when the nano-SiO_2 content is raised further, the tensile strength of SPN decreases, probably because the elastic collision of particle intensified, aggregation and phase separation are generated in composites, so a worse dispersion of the nanoparticles forms in the starch/PVA composites.[19]

The dependence of the elongation at break on the nano-SiO_2 content of the blend films is shown in Figure 2. There is a slight decreasing trend with an increasing content of nano-SiO_2, which is perhaps relative to the interfacial microstructure between the matrix and fillers. Owing to the presence of hydrogen bonds and covalent bonds, starch/PVA chains are easily connected to the surface of the adhered starch/PVA around the silica nanoparticles. Therefore, the interpenetrating network structure was formed to restrict the relative sliding between starch/PVA and nano-SiO_2 molecular.

Water absorption

As one of the major drawbacks in the use of a starch-based material is its water absorption tendency, any improvement in water resistance is therefore highly important. The water absorption of the SP and SPN films are shown in Figure 3. It can be easily found that the water absorption of the blend film decreased with an increase of nano-SiO_2 content. The water absorption of the SP film was 207.69% whereas the SPN3 had the lowest water

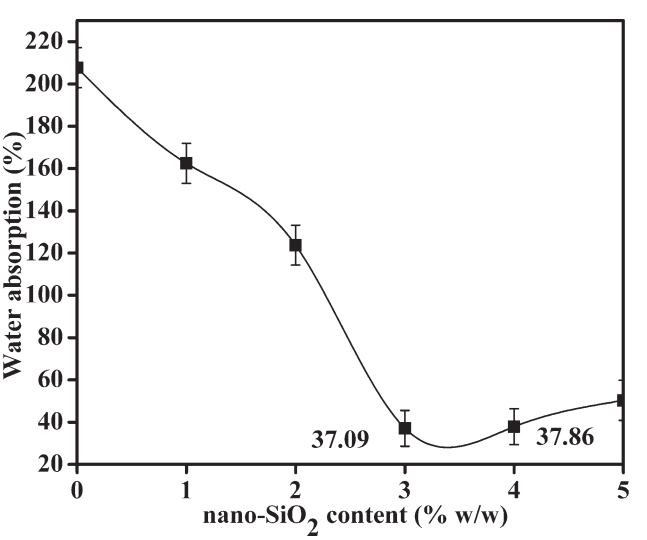

Figure 3 The dependence of the water absorption on the nano-SiO_2 content of blend films.

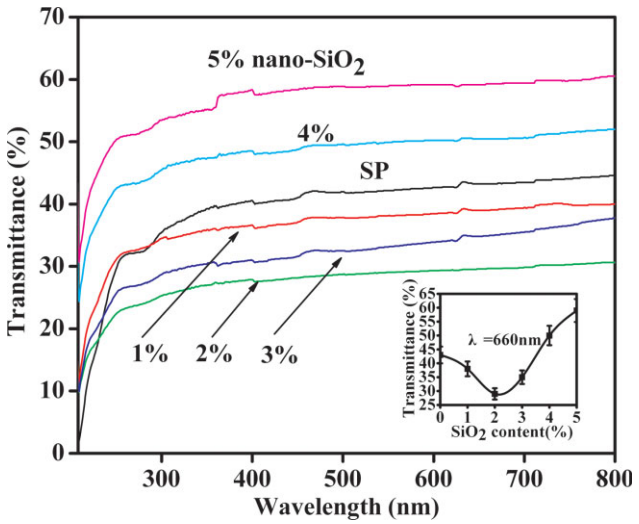

Figure 4 Transmittance variation of the hybrid films with different nano-SiO_2 content over a wavelength range of 200-800 nm. [Color figure can be viewed in the online issue, which is available at www.interscience.wiley.com]

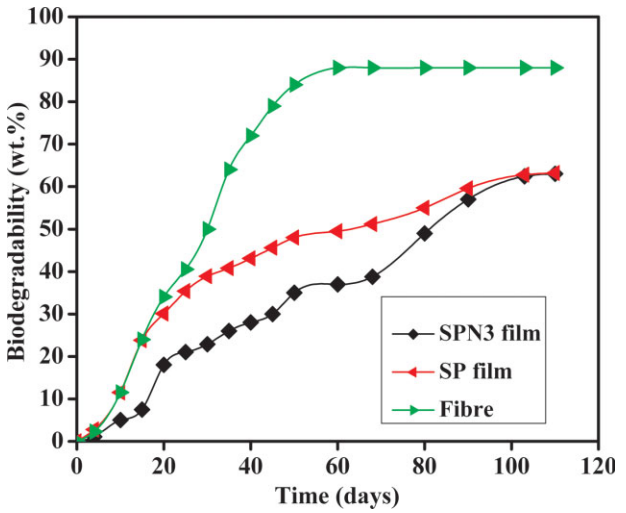

Figure 5 Biodegradability of the SPN3 film. [Color figure can be viewed in the online issue, which is available at www.interscience.wiley.com]

absorption at about 37.09%. When the nano-SiO_2 content varied from 3 to 5%, the water absorption of the SPN film increased, but it was still much lower than that of SP film. The reason was because of the network structure formed by combining nano-SiO_2 with starch/PVA, which prevented the water molecules from dissolving the SPN film and improved the water resistance of the film. However, the water absorption values of SPN films exhibited a slight increasing with nano-SiO_2 content increased further, what could be related to high surface energy and plenty of free hydroxyl groups of nano-SiO_2, and the surface energy and free hydroxyl groups might be beneficial to interact with water.

Transmittance

Figure 4 shows the transmittance of SPN films in the wavelength range of 200–800 nm. As shown in the inset (Fig. 4), the transmittance at 660 nm decreases from 43% of SP films to 29% of SPN films with 2% nano-SiO_2 content, and then gradually increases from 29 to 59% of the SPN films with 5% nano-SiO_2 content. It is because at low nano-SiO_2 content (<3%), the nano-SiO_2 particles are blended into starch/PVA chains to form an aggregation phase in the hybrid matrix. This leads to an decrease in the transparence of the hybrid film. At high nano-SiO_2 content (>3%), the nano-SiO_2 particle is isolated as a "dispersive" heterogeneous phase in the hybrid matrix, which results in a serious light scattering. This leads to a hazy thin film. SPN3 had the best optical transparence among all of the blend films, indicating that SPN3 has the best miscibility among the blend films.

Biodegradability

SPN3, presented the preferable properties in the above experiment, was chosen to do the research, fiber (poplar wood fiber) and SP film were used as reference substances and to confirm the validity of them. The biological decomposition rate of a starch-based biodegradable film modified by nano-SiO_2 is shown in Figure 5. From the figure, it can be seen that the biodegradability of the starch-based

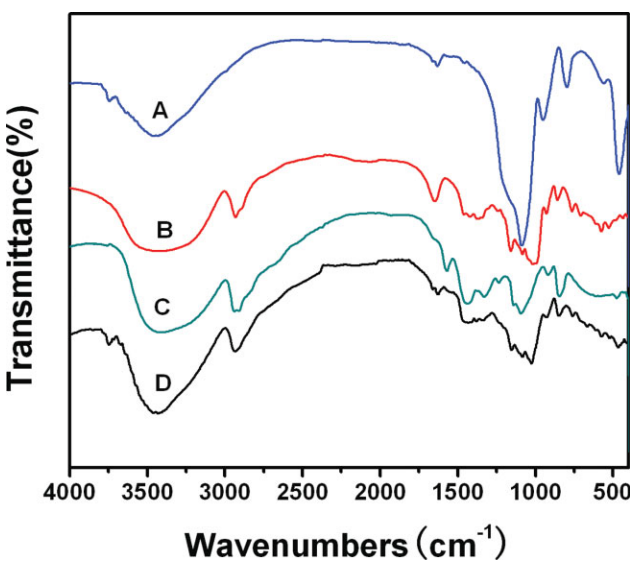

Figure 6 The IR spectrum of nano-SiO_2 (A), starch (B), PVA (C), and SPN3 film (D). [Color figure can be viewed in the online issue, which is available at www.interscience.wiley.com]

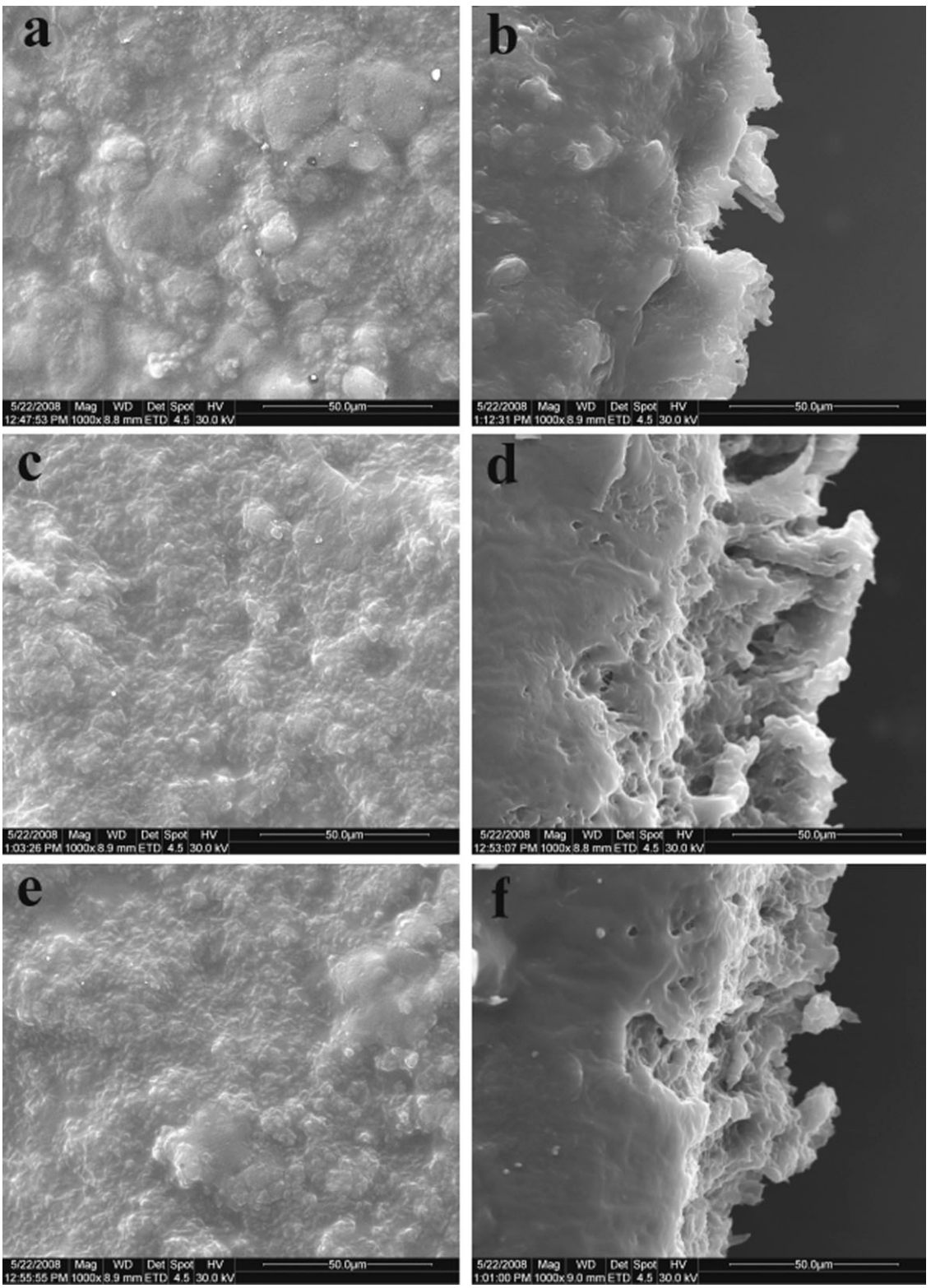

Figure 7 SEM images of the surface and cross sections of blend films (a) surface of SPN1; (b) cross section of SPN1; (c) surface of SPN3; (d) cross section of SPN3; (e) surface of SPN5; (f) cross section of SPN5.

biodegradable film was able to meet the demands of the ISO14855-1999; the addition of nano-SiO_2 had no influence on the biodegradability of the film as a whole. The biodegradation trend could be concluded from the test data. In the beginning, at 4 days, there was only a slow biodegradation rate at just 1.1%. Later on, the biodegradation became obvious and the rate reached 22.9% at 30 days. A slow

biodegradation period appeared during 31–68 days where the rate reached 38.8% at 68 days. However, the biodegradation rate rose significantly during 69–103 days where the rate became 62.4% at 103 days. Afterwards, there was a slow degradation, therefore, the SP and SPN3 exhibited the same biodegradation rate. Thus, the biodegradation of the film was a complicated process. In the early stage, because of the compact and homogeneous interpenetrating network structure of the film, the microbial had little influence on it. Yet, as the interaction of the microorganism and starch molecule increased, the biodegradation was accelerated. When the starch was almost fully degraded, the PVA was also further degraded but its speed was slower than that of the starch molecular; but under the condition of fixed composition, the PVA will exhibit the same biodegradation rate as starch at later stage. The weak biodegradability of PVA could be partly caused by the chemical structure of the PVA (unknown stereoregularity of hydroxyl groups) or by the degree of polymerization (comparably high molecular weight).

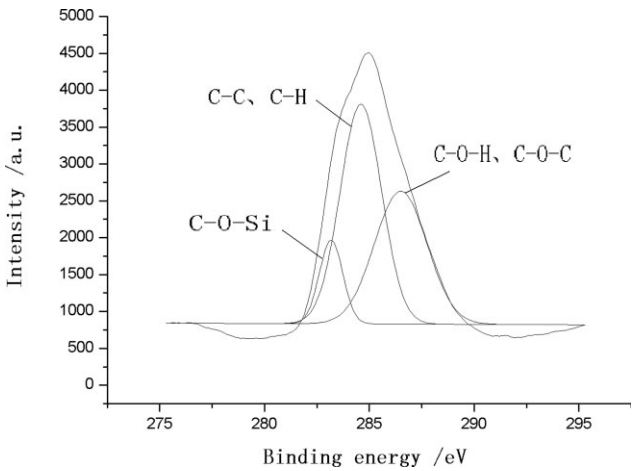

Figure 8 The spectra of SPN3 film deconvoluted into multiple subpeaks of C1S contained in different functional groups using the Gaussian-Lorentzian fit.

FTIR analysis

The IR spectra of nano-SiO_2 (A), starch (B), PVA (C), and SPN3 films (D) are shown in Figure 6. The strong and wide absorption band at 3447 cm^{-1} of the nano-SiO_2 (A) samples indicated that there were plenty of —OH on the surface of the nano-SiO_2. The absorptions near 1100 cm^{-1}, 810 cm^{-1}, and 470 cm^{-1} were attributed to the asymmetric stretching vibration, symmetric stretching vibration, and bending vibration of Si-O-Si, respectively.

From the spectra of starch (B), the strong and broad absorption peak at 3413 cm^{-1} was assigned to the characteristic absorption peak of the stretching vibration of —OH and the hydrogen bonds association in —OH groups. The bands at 1168 cm^{-1} and 1071 cm^{-1} were attributed to the stretching vibration of C—O in C—O—H groups, and the band at 1026 cm^{-1} was attributed to the stretching vibration of C—O in C—O—C groups. Meanwhile, the characteristic absorptions of starch also appeared at 1463 cm^{-1}, 1408 cm^{-1}, and 860 cm^{-1}.

For pure PVA (C), as with almost all organic compounds, an absorption band can be seen at 2911 cm^{-1} due to the stretching vibrations of CH and CH_2 groups. The bands attributed to the CH and CH_2 deformation vibrations were present at the 1300–1500 cm^{-1} range. Also very intensive, the broad hydroxyl band occurs at 3000–3600 cm^{-1} and an accompanying C—O stretching exists at 1000–1260 cm^{-1}.

In the IR spectrogram (D), the absorption peak of —OH was at 3420 cm^{-1} for the blend films of nano-SiO_2/starch. The peak shifted to a lower wave-number by 27 cm^{-1} compared with that of nano-SiO_2. The bands at 1159 cm^{-1} and 1089 cm^{-1} were attributed to the stretching vibration of C—O in C—O—H groups, and the band at 1022 cm^{-1} was attributed to the stretching vibration of C—O in C—O—C groups where all peaks shifted to a higher wave-number than that of starch. This indicated that the intermolecular hydrogen bonding of starch decreased with the addition of nano-SiO_2 and that the hydrogen bonding between nano-SiO_2 and starch was enhanced by the heat energy and high speed stirring.

Morphology of the films

Figure 7 shows the SEM images of the surfaces and cross sections of the films SPN1, SPN3, and SPN5. As to the surface image of SPN1 (a), most of the surface morphology had certain discontinuous zones and there were some assemble particles in the matrix. From the image of SPN3 (c), it was found that the shape of the surface morphology changed from this pattern to ordered, the surface morphology exhibited much more homogeneous and smooth. As to SPN5 (e), a homogeneous morphology was displayed and the assemble particles became small and uniform. The cross section images of films also showed that SPN3 had no obvious aggregations of nanocrystals and microphase separation, which indicated that good compatibility of the components and nano-SiO_2 with content of 3%.

XPS analysis

X-ray photoelectron spectroscopy (XPS) was used to characterize the nano-SiO_2 and NSP films. The XPS spectrograms are shown in Figure 8 and 9.

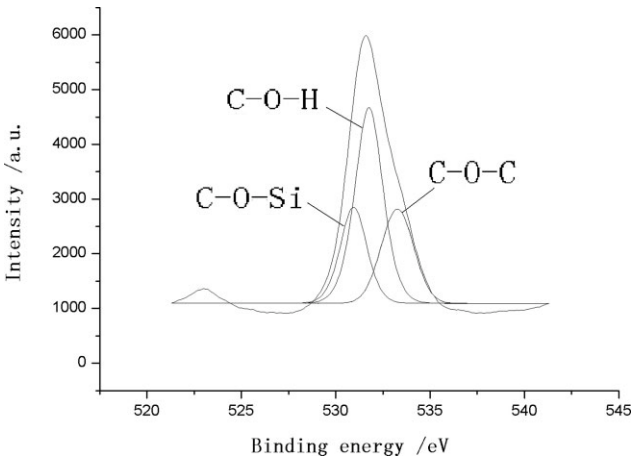

Figure 9 The spectra of SPN3 film deconvoluted into multiple subpeaks of O1S contained in different functional groups using the Gaussian-Lorentzian fit.

Figures 8 and 9 illustrated the narrow scan regions of C_{1s} and O_{1s} in SPN3 film, respectively. By peak fitting, peaks could be seen at around 283.2 eV, 284.6 eV, and 286.5 eV for C_{1s} in the SPN3 films (Fig. 8). This suggested the existence of three different environments. The peak at around 284.6 eV was attributed to the C_{1s} in the C—C and C—H groups, the peak at around 286.5 eV was due to the C_{1s} in the C—O—H and C—O—C groups, and the other peak at around 283.2 eV was the C_{1s} in the C—O—Si group. The results were in good agreement with the three states of the C—C (or C—H), C—O—H (or C—O—C), and C—O—Si in the SPN3 film. An analysis of the states of oxygen showed the peaks at around 531.76 eV, 533.27 eV, and 530.95 eV for O_{1s} (Fig. 9) in the SPN3 films, thus suggesting the existence of three different environments.[20] The peak at around 531.76 eV was attributed to the O_{1s} in the C—O—H group, the peak at around 533.27 eV was the O_{1s} in the C—O—C group, and 530.95 eV was the O_{1s} in the C—O—Si group. By combining all the XPS analysis results, the C—O—Si bond was found to be formed in nano-SiO_2/starch/PVA hybrid materials.

CONCLUSIONS

In this work, the results of the experiment show that the mechanical properties of the films are improved by addition of nano-SiO_2, the blend films appear the best tensile strength with 15.33 MPa, and the lowest water absorption with 37.09% at about 3 wt % of the nano-SiO_2 content, furthermore, the biodegradability of the SPN3 film meets the demands of the ISO14855 : 1999. The FTIR and XPS analysis indicated that the intermolecular hydrogen bond was formed in nano-SiO_2 and starch/PVA, and the strong chemical bond C—O—Si was also formed in nano-SiO_2/starch/PVA hybrid materials, The SEM analysis predicted that there was good miscibility between nano-SiO_2 and components in the blends when the nano-SiO_2 content was 3%. Meanwhile, the nano-SiO_2 and starch/PVA blends also formed a network structure to prevent the water molecular from dissolving the SPN film, which greatly increased the water resistance and mechanical properties of the film.

References

1. Mezzanotte, V.; Bertani, R.; Degli Innocenti, F.; Tosin, M. Polym Degrad Stab 2005, 87, 51.
2. Jayasekara, R.; Harding, I.; Bowater, I.; Christie, G. B. Y.; Lonergan, G. T. Polym Test 2004, 23, 17.
3. Bertuzzi, M. A.; Armada, M.; Gottifredi, J. C. J Food Eng 2007, 82, 17.
4. Bertuzzi, M. A.; CastroVidaurre, E. F.; Armada, M.; Gottifredi, J. C. J Food Eng 2007, 80, 972.
5. Parra, D. F.; Tadini, C. C.; Ponce, P.; Lugão, A. B. Carbohydr Polym 2004, 58, 475.
6. Chaichana, E.; Jongsomjit, B.; Praserthdam, P. Chem Eng Sci 2007, 62, 899.
7. Sun, S. S.; Li, C. Z.; Zhang, L.; Du, H. L.; Burnell-Gray, J. S. Eur Polym J 2006, 42, 1643.
8. Yang, H.; Zhang, Q.; Guo, M.; Wang, C.; Du, R, N.; Fu, Q. Polymer 2006, 47, 2106.
9. Zou, W. J.; Peng, J.; Yang, Y.; Zhang, L. Q.; Liao, B.; Xiao, F. R. Mater Lett 2007, 61, 725.
10. Follain, N.; Joly, C.; Dole, P.; Bliard, C. Carbohydr Polym 2005, 60, 185.
11. Xiao, C. M.; Yang, M. L. Carbohydr Polym 2006, 64, 37.
12. Zhai, M. L.; Yoshii, F.; Kume, T.; Hashim, K. Carbohydr Polym 2002, 50, 295.
13. Zhai, M. L.; Yoshii, F.; Kume, T. Carbohydr Polym 2003, 52, 311.
14. Shang, Y.; Peng, Y. L. Desalination 2008, 221, 324.
15. Zhang, S. J.; Yu, H. Q. Water Res 2004, 308, 309.
16. Baldev, R.; Annadurai, V.; Somashekar, R.; Madan, R.; Siddaramaiah, S. Eur Polym J 2001, 37, 946.
17. IDT ISO. Determination of the ultimate aerobic biodegradability and disintegration of plastic materials under controlled composting conditions-Method by analysis of evolved carbon dioxide. IDT ISO 14855, 1999.
18. Li, B.; Kennedy, J. F.; Jiang, Q. G.; Xie, B. J. Food Res Int 2006, 39, 544.
19. Xu, X. M.; Li, B. J.; Lu, H. M.; Zhang, Z. Appl Surf Sci 2007, 254, 1456.
20. Li, X. H.; Cao, Z.; Zhang, Z. J.; Dang, H. X. Appl Surf Sci 2006, 252, 7859.